The 2009 IEEE/RSJ International Conference on
Intelligent Robots and Systems
October 11-15, 2009 St. Louis, USA

New Likelihood Updating for the IMM Approach Application to Outdoor Vehicles Localization

Alexandre Ndjeng Ndjeng, Dominique Gruyer and Sébastien Glaser

Abstract— **This paper presents the problematic of outdoor vehicle localization under the IMM (Interacting Multiple Model) approach. The IMM is now a well known modular approach, which is based on the discretization of the vehicle evolution space into simple maneuvers, represented each by a simple dynamic model such as constant velocity or constant turning etc. This allows the method to be optimized for highly dynamic vehicles. Unfortunately classical IMM shows some drawbacks concerning some real time multi sensors applications. In this work, we focus on outdoor vehicle localization with asynchronous sensors in order to report these drawbacks and then propose a new solution. Many tests carried out with simulated and real data confirm the interest for using such a solution in our applications.**

I. INTRODUCTION

Reducing vehicles localization error while increasing robustness is an always increasing requirement for the development of the driving assistant systems. In order to reach this goal, multi sensors data fusion techniques have been used since some years [1], [2].
Among the methods of road vehicles localization now widely presented in the literature, the IMM (Interacting Multiple Model) approach, in addition to guarantee a greater robustness to model unmatching, makes it possible to identify the current dynamics through the various models activation probabilities assessment. In fact, the use of this method contributed to improve the localization robustness and integrity [2], [3], through multiple model adaptation. The IMM was mainly applied to solve problems of objects tracking with strong nonlinear dynamics [4], [5].

However, using the traditional IMM algorithm for road vehicle localisation as presented in [3] or [6] can reveal important drawbacks coming from various sources of error. Firstly, noisy sensors data used as inputs can cause the system drift. Secondly, a wrong Markovian transition matrix, which means wrong switching parameters, can provide a wrong model probabilities evaluation. Nevertheless, these problems can be solved either through sensors data preprocessing (denoising, unbiasing, etc.), or through stability tests on the system [4] However, the most critical drawback which is treated in this work concerns the probability regime updating when exteroceptive data are absent. Usually, the probabilities are updated by using the models likelihoods, derived from innovations which are obtained only in presence of exteroceptive sensors data, e.g. GPS. In case of GPS outage, for example, probabilities are not updated and the system modeling will be probably wrong. Commonly used solution is to synchronize the used sensors to the GPS frequency [3]. Unfortunately, the frequency of this sensor is weak in comparison with the inertial sensors or odometers. In addition, the quality of the GPS positioning depends on the conditions of the environment, and can undergo maskings (in a forest, a tunnel or an urban canyon). A robust solution to this problem is proposed in this work. In such situations, we use proprioceptive sensors data in order to design a new system modeling, which will contribute to update various model probabilities.

The authors are with the combined INRETS/LCPC Vehicle - Infrastructures - Driver Interactions Research Unit (LIVIC), 14, route de la minière, Bât 824, 78000 Versailles France
Corresponding author email: *alexandre.ndjeng@inrets.fr*

This paper is shared into three parts. The next section is dedicated to the presentation of the traditional IMM estimator, and especially the parameters setting and application to vehicle localization with drawbacks. Then the second part presents the new likelihood updating approach that we propose. Finally a conclusion is given.

II. REVIEW OF THE TRADITIONAL IMM APPROACH

A. Formulation

The limitations of traditional mono model Kalman filter derivatives bring up a need to get a more robust estimator, which is not based on the system model linearization [1]. Instead, several simple and linear kinematic models are implemented in parallel. The process model equation for the i^{th} system approximation from a set of m vehicle candidate models is described in equation 1, where $f^{(i)}$ is the i^{th} process function:

$$X_{k|k-1}^{(i)} = f^{(i)}(X_{k-1|k-1}^{(i)}, u_k^{(i)}, w_k^{(i)}) \quad i \in [1 \cdots m] \tag{1}$$

and the observation model for this i^{th} filter is given by equation 2, where $h^{(i)}$ is the i^{th} measurement function,

$$Y_k^{(i)} = h^{(i)}(X_{k|k-1}^{(i)}, v_k^{(i)}) \tag{2}$$

$X_{k|k-1}^{(i)}$ is the predicted state vector given by the i^{th} model at time index k:
$X_{k|k-1}^{(i)} = [x_{k|k-1}^{(i)}, y_{k|k-1}^{(i)}, \dot{x}_{k|k-1}^{(i)}, \dot{y}_{k|k-1}^{(i)}]'$ where $[x_{k|k-1}^{(i)}, y_{k|k-1}^{(i)}]'$ is the position vector and $[\dot{x}_{k|k-1}^{(i)}, \dot{y}_{k|k-1}^{(i)}]'$ is the speed vector. $u_k^{(i)}$ represents the inputs at time k. $w_k^{(i)}$ and $v_k^{(i)}$ are the process and measurement noises, which are assumed white and Gaussian. $Y_k^{(i)}$ is the measurement vector and $(.)'$ represents the transpose operator.

B. Implementation

The jumps between the various system models are determined following a Markov chain process [7]. The IMM algorithm is implemented in four main steps, which are summarized in the following:

- **Interaction:** Each filter estimate is mixed with others using a predicted model probability and the Markov transition probability π_{ji}.
- **Specific Filtering:** The filter state and covariance matrix are predicted, using the mixed states, covariances and the filter inputs. Then, the corrective step including the computation of the measurement residual, the residual covariance, the estimate and its covariance are computed.
- **Model Probability update:** Each predicted model probability is updated with respect to the measurement residual, once an exteroceptive (GPS) measurement is available. The mode likelihoods $\Lambda_k^{(i)}$ are computed in equation 3, and then the model probabilities $\mu_{k|k}^{(i)}$ are updated in equation 4.

$$\Lambda_k^{(i)} = \frac{\exp[-0.5(\tilde{y}_k^{(i)})'(S_k^{(i)})^{-1}\tilde{y}_k^{(i)}]}{|2\pi S_k^{(i)}|^{1/2}} \quad (3)$$

$$\mu_{k|k}^{(i)} = \frac{\mu_{k|k-1}^{(i)}\Lambda_k^{(i)}}{\sum_j \mu_{k|k-1}^{(j)}\Lambda_k^{(j)}} \quad (4)$$

  where $\mu_{k|k-1}^{(i)}$ is the i^{th} model predicted probability, $\tilde{y}_k^{(i)}$ measurement residual and $S_k^{(i)}$ the residual covariance matrix.
- **Estimate fusion:** The filter output estimate $\hat{X}_{k|k}$ and its covariance matrix $P_{k|k}$ are computed from a fusion of the weighted state estimates.

More details on this filter implementation can be found in [2]–[6].

In order to perform the vehicle localization with IMM, five different vehicle models are used. These models include the *Constant Velocity Model* (CV) for the free motion modes. The longitudinal dynamics can be described by the *Constant Acceleration Model* (CA) model. For the lateral dynamics, we use the constant yaw rate with constant velocity model, named the *Constant Turn Model* model (CT). Moreover, a *Constant Stop* (CS) and a *Constant Rear* (CR) models are used to describe stops and backwards driving situations, respectively. Details on these models are found in [3], [8] and [6].
Moreover, [8] and [9] present various ways to setup the IMM filter, in terms of Markov transition matrix and the noise covariance matrices.

C. Application to outdoor Vehicles Localization

Traditional IMM gives interesting results for outdoor vehicle localization, particularly when provided data are synchronized and available at the same frequency [2], [6]. In such cases, the various model probabilities are updated at every time index, because the required updating data are available. But when exteroceptive data (e.g. GPS) are absent, in case asynchronous sensors are being used, these probabilities are not updated. Hence defaults appear in the system, as shown in the following experiments.

Scenario 1:
The experimental results that are presented in this section are derived from two different scenarios. The first scenario focuses on some parking maneuvers with stops, forward and backward driving situations. This scenario describes a complex situation: in this experiment, the embedded sensor architecture provided data at different frequencies (accelerations ($8Hz$), rotation rates ($8Hz$), odometric speed ($25Hz$) and GPS position ($5Hz$)).

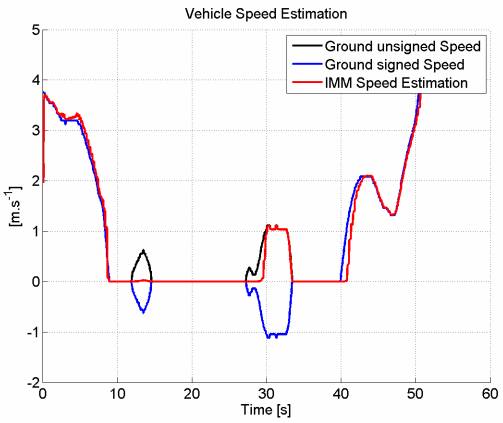

Fig. 1. Speed estimation : scenario 1

This scenario shows two backward driving stages (signed speed is negative, see figure 1). By comparing the vehicle speed with probabilities in figure 2 we can see an important correlation. The various vehicle maneuvers can be globally identified, except the first backward driving step at very low speed ($\approx 0.6m/s$). During stop situations the CS model probability is the highest, around 0.99. Similarly, the CR model probability is around 0.90 during the second backward driving step.
The speed estimation is globally acceptable. The maximum speed error is about $0.5m.s^{-1}$, this value is obtained when the vehicle switches from a stop to a forward or a backward driving state (at time $12s$, $28s$ and $40s$). This deviation is introduced by the system inertia when switching from a state to another, and worsened by a lower frequency probabilities updating. These probabilities describe staircases, since they are updated every $200ms$ while the system output is available every $40ms$.

Scenario 2:
The second scenario is derived from simulations. It describes a complex trajectory (straight lines and turns) which is traversed in 200 *seconds* as shown in figure 3. GPS, IMU and

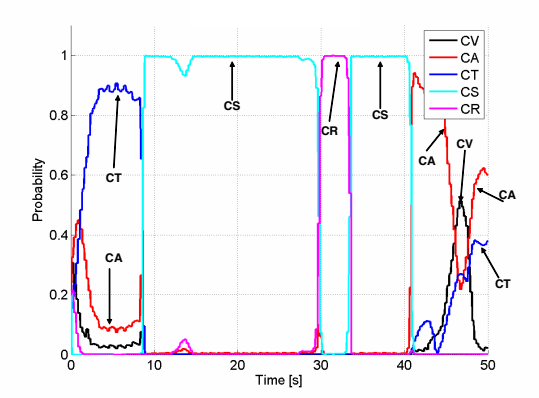

Fig. 2. Probabilities : scenario 1

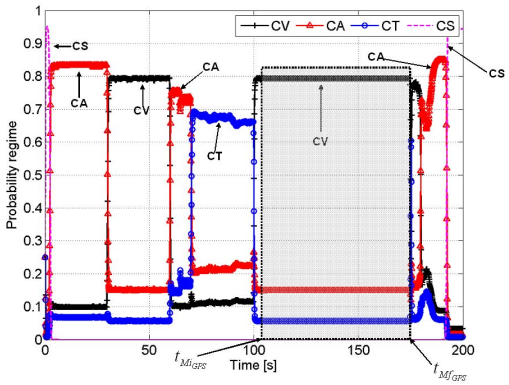

Fig. 4. Probabilities: scenario 2

Odometer data are simulated and provided at the frequency of $5Hz$. GPS data have additional Gaussian white noise with $3m$ standard deviation.

After the first turn, a GPS outage is simulated between $t_{Mi_{GPS}} = 105s$ and $t_{Mf_{GPS}} = 175s$ (see figure 3). During this period, models probabilities are not updated and IMM runs only with proprioceptive sensors data.

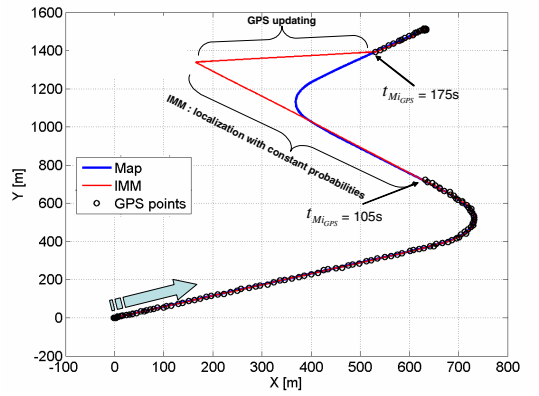

Fig. 3. Simulated test track: scenario 2

Figure 3 shows the traditional IMM positioning output. At time $t_{Mi_{GPS}}$, the vehicle follows a straight line at constant speed, thus the CV model probability is the most important, about 0.8. During the GPS outage, various models probabilities remain constant (see figure 4), so the CV remains the dominant model. This directly derives into a wrong modeling of the second turn. In such a situation, traditional IMM cannot solve the localization problem on a complex track. Therefore in order to implement a reliable IMM for outdoor vehicles localization, it is necessary to update the various model likelihoods even when only proprioceptive data are available. Our solution in order to solve this issue is described in the next section.

III. Likelihood Updating with Proprioceptive Sensors

A. Introduction

In outdoor vehicle localization applications, the use of asynchronous sensors data enables to exploit almost all the collected data without re-sampling. As shown in the previous section, it is difficult to use traditional IMM with asynchronous sensors for real time vehicle localization. In fact, the model likelihoods remain constant as long as GPS data are absent. However, it is possible to evaluate these likelihoods with only proprioceptive sensors, as we will show in the following. Considering the same evolution models that previously, we define new non homogeneous constrained state vectors, which result from the modeling of the proprioceptive sensors behaviors. For example, the constrained constant acceleration state vector is derived from accelerometers global behaviors.

B. Proprioceptive sensors behavior modeling

For this new system modeling, proprioceptive sensors global behavior is used to describe the system maneuvers. The various sensors behavior modeling is set in the normalized the interval $[-1,\ 1]$. In order to refine this modeling, sub-models are defined, represented by normal distributions centered at m_i (the most likely point for the given sub-model), with variance σ_i. The resulting sensor behavior modeling therefore obeys the following scheme.

- ***Sensor behavior modeling for data at zero,*** d_0***:*** in such a situation, the sensor behavior is represented by a normal distribution centered at 0, with the variance $\sigma_{sub-model}$: this is the central distribution in figure 5.
- ***Sensor behavior modeling for data close to zero,*** d_m ***(absolute value):***
  Many normal distributions (sub-models) are set around 0 according to the following rule: given two sub-models g_0 and g_1 with respective parameters (m_0, σ_0) (known values) and (m_1, σ_1) (to be determined): in order to avoid local minima, while describing the global sensor behavior model, it is suggested that g_0 and g_1 should have as intersection, the most likely point of g_1,

combined to a fraction $\alpha > 1$, between both variances. Therefore distribution g_1 can be obtained as a function of m_0, σ_0 and α, according to equations 5

$$\left| \begin{array}{lcl} \sigma_1 & = & \alpha\sigma_0 \\ and & & \\ m_1 & = & m_0 + \sigma_0\sqrt{2\log\alpha} \end{array} \right. \quad (5)$$

The resulting distributions are represented in figure 5. In this example, α equals 1.5. The values of alpha are experimentally determined and constitutes the characterizing parameters of the modeling. Indeed, more α is close to 1, more the variances of successive sub-models centers are close to one another. In this case, the number of distributions becomes important and the system is not discriminating. In our experiments, $\alpha = 1.5$ gave the best results.

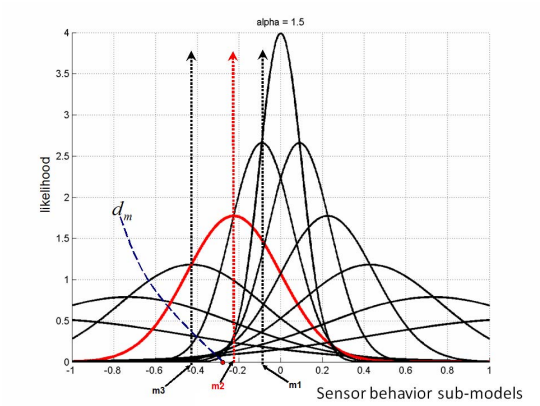

Fig. 5. Sensor behavior modeling for measurements close to 0: d_m, $\alpha = 1.5$

- ***Sensor behavior modeling for data greater than*** 0***,*** d_M ***(absolute value):***
  The sub-models are obtained in a similar way as in the previous case. The difference is that for the given normal distributions g_0 and g_1, the intersection should be the most likely point of g_0, then $0 < \alpha < 1$. Knowing g_0, distribution g_1 is obtained according to formulas in equations 6.

$$\left| \begin{array}{lcl} \sigma_1 & = & \alpha\sigma_0 \\ and & & \\ m_1 & = & m_0 + \alpha\sigma_0\sqrt{-2\log(\alpha)} \end{array} \right. \quad (6)$$

  An illustration is given in figure 6. For our experiments, $\alpha = 0.6$ gave the best results, in terms of switching regime from one models to another.

For a given measurement, the chosen sub-model should provide its maximum likelihood. In figure 5 for example, the chosen distribution for d_m is centered at m_2 (red colored); and in figure 6 the chosen distribution for d_M is centered at m_2 (red colored). Consequently, the following models are set, as a derivation of various sensors behavior modeling:

$$Low\ \ speed(Odometer): \quad V_{mk} \rightsquigarrow \mathcal{N}(m_V^{(k)}, \sigma_{mV}^{(k)}) \quad (7)$$

$$High\ \ speed(Odometer): \quad V_{Mk} \rightsquigarrow \mathcal{N}(M_V^{(k)}, \sigma_{MV}^{(k)}) \quad (8)$$

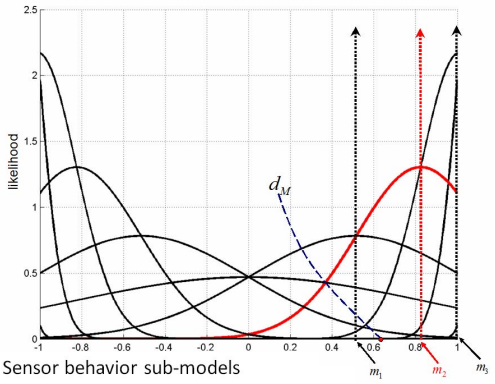

Fig. 6. Sensor behavior modeling for measurements greater than 0: d_M, $\alpha = 0.6$

$$Longitudinal\ \ accelerometer: \quad \gamma_{xk} \rightsquigarrow \mathcal{N}(m_{\gamma_x}^{(k)}, \sigma_{\gamma_x}^{(k)}) \quad (9)$$

$$Lateral\ \ accelerometer: \quad \gamma_{yk} \rightsquigarrow \mathcal{N}(m_{\gamma_y}^{(k)}, \sigma_{\gamma_y}^{(k)}) \quad (10)$$

$$Yaw\ \ rate(Gyro): \quad \omega_k \rightsquigarrow \mathcal{N}(m_{\omega}^{(k)}, \sigma_{\omega}^{(k)}) \quad (11)$$

The center and variance values of these sub-models are used to define the subsequent constrained state vectors and the covariance matrices. In fact, the centers of these distributions can be gathered in only one constrained state vector that describes the system : $X_k^c = \left[m_{\gamma_x}^{(k)}\ m_{\gamma_y}^{(k)}\ m_{\omega}^{(k)}\ mM_V^{(k)}\right]'$, where $mM_V^{(k)}$ is the speed component (low and high speed) derived from odometer behavior modeling. The other terms are defined from equations 7 to 11. Consequently, each model being a partial representation of the total evolution space, will have a state vector which is a partition of the total vector X_k^c.

C. Proprioceptive sensors-based System Modeling

This new system modeling is based on the hypothesis that the vehicle dynamics can be represented by both inertial and signed vehicle speed measurements: accelerations γ_x and γ_y, yaw rate ω and vehicle signed speed V. Therefore, the following rules and constrained models (state vectors $X^{c(i)}$ and covariance matrices $P^{c(i)}$) are set and used to describe various vehicle maneuvers.

- An important longitudinal and lateral acceleration derives in an constrained accelerated evolution mode: *cCA model*

$$X_k^{cCA} = [m_{\gamma_x}^{(k)}\ m_{\gamma_y}^{(k)}]' \quad (12)$$

$$P_k^{cCA} = q_k^{(CA)} \begin{pmatrix} \sigma_{\gamma_x}^{2(k)} & 0 \\ 0 & \sigma_{\gamma_y}^{2(k)} \end{pmatrix} \quad (13)$$

- An acceleration vector close to 0, combined with a weak yaw rate describe a straight line evolution at constrained constant speed: *cCV model*

$$X_k^{cCV} = [m_{\gamma_x}^{(k)}\ m_{\gamma_y}^{(k)}\ m_{\omega}^{(k)}]' = [0\ 0\ 0]' \quad (14)$$

$$P_k^{cCV} = q_k^{(CV)} \begin{pmatrix} \sigma_{acc\,\gamma_x}^2 & 0 & 0 \\ 0 & \sigma_{acc\,\gamma_y}^2 & 0 \\ 0 & 0 & \sigma_{gyro\,\omega}^2 \end{pmatrix} \quad (15)$$

where $\sigma^2_{acc\,\gamma_x}$ is the variance on X-axis accelerometer sub-model, $\sigma^2_{acc\,\gamma_y}$ the variance on Y-axis accelerometer and $\sigma^2_{gyro\,\omega}$ denotes the gyro sub-model variance.

- An important lateral acceleration combined with a high yaw rate derives in a constrained turn: *cCT model*

$$X_k^{cCT} = [m_{\gamma_y}^{(k)}\ m_{\omega}^{(k)}]' \tag{16}$$

$$P_k^{cCT} = q_k^{(CT)} \begin{pmatrix} \sigma_{\gamma_y}^{2(k)} & 0 \\ 0 & \sigma_{\omega}^{2(k)} \end{pmatrix} \tag{17}$$

- A non zero negative speed implies a constrained backwards driving scenario: *cCR model*

$$X_k^{cCR} = [-M_V^{(k)}] \tag{18}$$

$$P_k^{cCR} = q_k^{(CR)} \sigma_{MV}^{2(k)} \tag{19}$$

- A zero acceleration vector, a zero yaw rate and a near to zero vehicle speed describe a constrained stop: *cCS model*

$$X_k^{cCS} = [m_{\gamma_x}^{(k)}\ m_{\gamma_y}^{(k)}\ m_{\omega}^{(k)}\ m_V^{(k)}]' = [0\ 0\ 0\ m_V^{(k)}]' \tag{20}$$

P_k^{cCS} is very similar to P_k^{cCV}. However, this covariance matrix also includes a term derived from the odometer behavior modeling: $\sigma_{mV}^{2(k)}$.

D. New model likelihoods computation

1) Measurement models: The various system measurement models are defined. These models depend on the sensors that are used to describe every maneuver of the vehicle described by a constrained evolution model. In this new approach, we define the observation vectors $Y_k^{(i)}$ as the measurement vector from exteroceptive sensors, used for the given sensors behavior. The covariance matrices of the measurement noise $R_k^{(i)}$ is derived from corresponding sensors errors.

2) Likelihoods computation formulas: Given a specific filter i, considering the above proprioceptive sensors behavior modeling, the likelihood is obtained according to the formula in equation 21.

$$\Lambda_k^{c(i)} = \frac{-0.5(\tilde{y}_k^{c(i)})'(S_k^{c(i)})^{-1}\tilde{y}_k^{c(i)}}{\sqrt{2\pi \det(S_k^{c(i)})}} \tag{21}$$

where $\tilde{y}_k^{c(i)}$ is the i^{th} constrained model innovation

$$\tilde{y}_k^{c(i)} = Y_k^{c(i)} - X_{k|k-1}^{c(i)} \tag{22}$$

and $S_k^{c(i)}$ the i^{th} innovation covariance matrix

$$S_k^{c(i)} = P_k^{c(i)} + R_k^{c(i)} \tag{23}$$

3) System output computation: Once the various constrained model likelihoods have been computed, these values are directly affected as the traditional model likelihoods : $\Lambda_k^{(i)} \leftarrow \Lambda_k^{c(i)}$. Therefore, the model probabilities are obtained according to equation 4.

Finally, the system output is computed as in the traditional IMM approach, using MMSE and MSE estimators, as described in [8].

E. Application to vehicle localization

The new system modeling presented above was applied to both scenario 1 and scenario 2. As shown in the following, by improving the model probabilities estimation in absence of GPS, the IMM position and speed estimations were improved.

Scenario 1:

Figure 7 represents the probability regime derived from the constrained system evolution modeling, based only on the proprioceptive noisy sensors data. From this figure, it is possible to identify the various vehicle evolution modes. This means, that the constrained evolution model probabilities obtained with IMU and Odometer are globally very similar to those obtained with GPS (see figure 2). Exception appears around the first stop around 10s. At this point, the constrained modeling allows to identify the slowing down maneuver before the stop, as well as the short backward driving after this stop.

Consequently, the speed estimation shown in figure 8 is better than that obtained when only GPS is used to update likelihoods. We now observe almost no deviation when the vehicle moves from a stop situation.

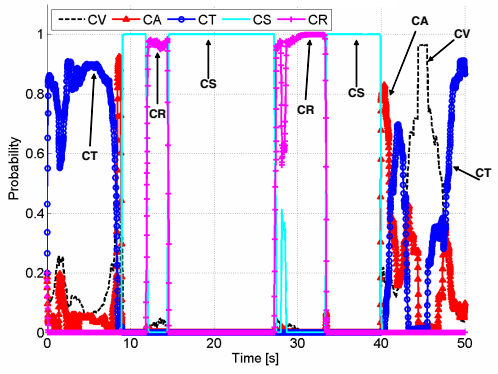

Fig. 7. IMU-Odometer based probabilities: scenario 1

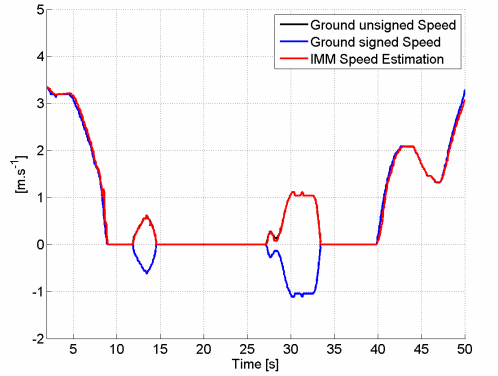

Fig. 8. IMM speed estimation: scenario 1

Scenario 2:

As shown in figure 9, it is remarkable that by using the

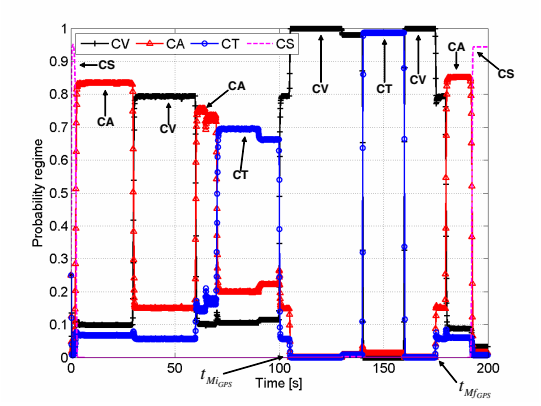

Fig. 9. GPS-IMU-Odometer based probabilities: scenario 2

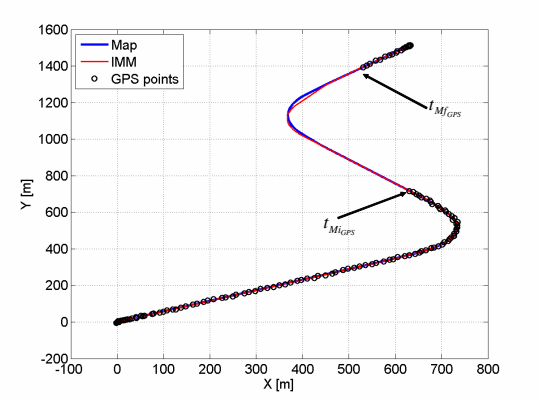

Fig. 10. Positioning with non constant mode likelihoods: scenario 2

constrained system modeling presented above, the second turn that occurs during GPS outage is clearly identified (around point 150*s*). This figure differs from figure 4 through the Constant velocity and Constant Turn model probabilities between $t_{Mi_{GPS}}$ and $t_{Mf_{GPS}}$. With system constrained modeling and the proprioceptive sensor-based likelihood computation, these model probabilities are not constant during the GPS outage. This period is characterized by a constant speed and a turn. Accordingly, the CV and CT models probabilities alternate. With a better evaluation of these model probabilities, the IMM-based vehicle positioning is improved (see figure 10). In fact, with the new system modeling, we don't observe the system drift and the IMM output trajectory is very close to the reference, even during the GPS outage.

IV. Conclusion

This paper has presented a novel approach for IMM mode likelihoods updating by using only proprioceptive sensors data. Usually in the autonomous vehicles applications, the mode likelihoods are obtained through model innovations computation, using a GPS position as real observation. Unfortunately in outdoor environments or real time safety applications, many situations can hinder a continuous likelihoods updating. In this paper two limitations are shown: firstly, a low GPS frequency can derive in low frequency likelihoods updating, with probabilities having staircases shape; secondly, a GPS outage or GPS signal blocking can cause the system drift when a nonlinearity occur during this outage.

In order to overcome these limitations, a new system modeling was proposed and applied to outdoor vehicle localization. This method uses proprioceptive sensors behavior modeling in order to design new models, that describe constrained evolution modes. With this approach, it was possible to identify various system evolution modes and to estimate the probabilities with or without GPS data. The resulting IMM algorithm that is used for a more robust outdoor vehicles localization has two ways for likelihood updating: in presence of GPS data, traditional IMM is applied; in absence of GPS data, the new modeling with constrained evolution modes is used.

V. Acknowledgment

This work is completed within the POSITIONING, MAPS & LOCAL REFERENCING sub-project (POMA) in the European project CVIS.

References

[1] S. J. Julier, *Process Models for the Navigation of High Speed Land Vehicles*. PhD thesis, University of Oxford, Departement of Engineering Science, 1997.

[2] R. T. Moreo, A. Z. Izquierdo, B. U. Minarro, and A. F. G. Skarmeta, "High-integrity IMM-EKF-based road vehicle navigation with low-cost gps/sbas/ins," *IEEE Tans. on Intelligent Transportation Systems*, vol. 8, no. 3, pp. 491–511, 2007.

[3] A. N. Ndjeng, S. Glaser, and D. Gruyer, "A multiple model localization system for outdoor vehicles," in *IEEE/Intelligent Vehicles Symposium*, (Istanbul), June 2007.

[4] S. Blackman and R. Popoli, *Multitarget-Multisensor Tracking: Advanced Applications*. Norwood,MA: Artech House, 1999.

[5] X. R. Li and V. P. Jilkov, "Survey of maneuvering target tracking. part 5: Multiple model methods," *IEEE Transactions on Aerospace and Electronic Systems*, vol. 41, no. 4, 2005.

[6] A. N. Ndjeng, D. Gruyer, and S. Glaser, "Low cost sensors ego localization with IMM approach for unusual maneuvers," in *Int. Conf. on Intelligent Transportation Systems IEEE/ITSC*, (Beijing, China), 12-15 Oct. 2008.

[7] H. A. P. Blom and Y. Bar-Shalom, "The interacting multiple model algorithm for systems with markovian switching coefficients," *IEEE Trans. on Aut. Control*, vol. 33, no. 8, pp. 780–783, 1988.

[8] X. R. Li and V. P. Jilkov, "Survey of maneuvering target tracking. part 1: Dynamic models," *IEEE Transactions on Aerospace and Electronic Systems*, vol. 39, pp. 1333–1364, Oct 2003.

[9] Y. Bar-Shalom, *Multitarget-Multisensor Tracking: Applications and Advances*, vol. II. Norwood, MA: Artech House, 1992.